# DIFFRACTION STUDIES FOR STRUCTURAL ANALYSIS OF LASER SYNTHESIZED CARBON NANOPOWDER

I. Morjan[a], I. Sandu[a], I. Voicu[a,*], I. Pasuk[b], R. Alexandrescu[a], T.C. Fleaca[a], F. Dumitrache[a], I. Soare[a], E. Popovici[a], and B. Rand[c]

[a] *National Institute for Lasers, Plasma and Radiation Physics, Laser Department, P.O. Box MG-36, R-76900 Bucharest, Romania*

[b] *Research Institute for Electrical Engineering-Advanced Research, 313 Splaiul Unirii St., 74204 Bucharest, Romania*

[c] *Institute for Materials Research, School of Process, Environmental and Materials Engineering, University of Leeds, Leeds LS29TT, U.K.*

*Corresponding author:* ivoicu@ifin.nipne.ro

**Abstract**

The laser pyrolysis of a hydrocarbon-based mixture is a suitable method for the synthesis of soot containing different carbon nanostructures. Precursors as ethylene, acetylene or benzene were used either in resonant or non-resonant (with $SF_6$ as energy transfer agent) laser pyrolysis processes. The soot morphology depends on the gas mixture and experimental parameters. The formation of some nanostructures is related to the presence of heteroatom in the reactants. The presence of oxygen is essential in obtaining soot particles having considerable curved-layer content. Oxidation reactions could be responsible for the soot morphology change from a turbostratic structure to a fullerene-like one. The presence of sulfur and fluorine, released by $SF_6$ dissociation could also alter the particles' structure. Diffraction studies on synthesized samples and other complementary methods of investigation allow putting into evidence changes in the soot morphology.

**Introduction**

The field of carbon nanomaterials is intensively studied as their potential use is considered in material science. Among other synthesis techniques, research tends to focus on pyrolysis, which means decomposition by heat supplied by flame combustion[1], laser[2, 3] or another general heat source. The high temperature gradients and fast reaction time involved in the process lead to very fine powders with uniform and controllable particle size distribution and make laser pyrolysis a versatile and efficient method for the synthesis of carbon nanopowders. The continuous synthesis method by laser pyrolysis of hydrocarbon-based mixture uses a CW $CO_2$ laser as an energetic controlled source for the heat supply to the chemical system and provides the possibility of a continuous method of production. The process is based on the interaction between laser radiation and at least one of the gaseous/vapor reactant. Hydrocarbons as ethylene (85,7 % C/mole), acetylene (92,3% C/mole) and benzene (92,3 % C/mole) were used either in resonant laser pyrolysis process (when precursor like ethylene -$\nu_7 = 949\ cm^{-1}$- absorbs laser radiation -$944\ cm^{-1}$-) or in no resonant process, when precursor doesn't absorb laser radiation and it was necessary to introduce an energy transfer agent. In such a sensitized system, small quantities of $SF_6$, whose main vibration frequency

is $\nu_3$ = 947 cm $^{-1}$ (overlapping the emission line of the $CO_2$ laser near 10,6 μm), play the role of the energy transfer agent. This energy transfer agent can either react or interfere through its decomposition products (sulfur or fluorine), and make difficult the control of the final particle morphology through the appropriate experimental parameters. The positive role of halogen additions and its thermally and photo chemically unstable halogenated intermediate species is suggested to improve the formation of some carbon nanostructures[4]. Also, the presence of oxygen allows the formation of fullerene-like nanostructures in that it is an important factor determining their formation, when polycyclic aromatic hydrocarbons participate in soot nucleation[5]. The nitrous oxide was chosen as oxidizer due to its low dissociation energy when, because of the high temperature involved in the process, it is readily decomposed and could have a more oxidizing character in the destruction of hydrocarbon and in reaction with precursors of final product. Focusing, in the context of necessary presence of these heteroatom in the gas composition, on the present questions concerning the rational synthesis of nanostructures with controlled dimensionality, size and potentially properties, the aim of the work was to investigate, mainly by diffraction methods, significant changes in soot morphology produced by these, sometimes unavoidable, atoms of oxygen, fluorine or sulfur.

**Experimental**

Reactive gas mixtures based on ethylene, acetylene or benzene with ethylene and sulfur hexafluoride as sensitizers and nitrous oxide as oxidizer were used. Both $N_2O$ and $SF_6$ were controlled as C/O and C/F atomic ratio, respectively. The experimental installation was composed by a continuous wave $CO_2$ laser (1 kW, $\lambda$=10.6 μm), a stainless steal flux reactor, gas and pressure control systems and a powder recovery trap. The interaction laser beam-reactive gas produces a bright sooting flame. Reaction products are formed by dissociation and radical reactions and by fast cooling precipitate under the form of very fine, solid particles with uniform and controllable size distribution. Laser power was varied from 400 to 900 W and pressure in the range of 400-900 mbar. Argon was used as a carrier gas for benzene vapors. The final particle morphology could be controlled by experimental parameters, with the goal to obtain different carbon nanostructures, from amorphous carbon up to those characterized by a high degree of curvature. Different experiments were performed by varying one parameter and trying to keep all the others constant.

The powder characteristics were investigated by electron transmission microscopy, TEM (coupled with EDAX and/or SAED, HREM) using a Philips FEGTEM 200 microscope with a Gatan 666 detector for electron energy loss spectroscopy (EELS) analysis. X-ray diffraction (XRD) spectrometry was performed with a Bruker D8 ADVANCE X-ray diffractometer; and IR spectra of soot samples were obtained with a SPECORD 75 IR spectrometer. Raman spectroscopy was performed using a Raman TM$^{2001}$ apparatus; 785 nm wavelength in a 180° backscatter configuration and a 30 s integration time.

Elemental chemical analysis of S, C and N were performed by Exhalograph - Haereus apparatus for gas determination in solids while fluorine was quantified by solving in alkaline melts and titration.

**Results and discussion**

At the high temperature of the laser pyrolysis process, the reactants are expected to dissociate after collision energy transfer from the vibrationally excited molecules of the sensitizer. It was shown that in these specific experimental conditions, the $SF_6$ sensitizer could undergo different degrees of dissociation and also reactions with other species[5]. The decomposition is probably enhanced because, in the presence of hydrogen, it requires less energy[6] and the temperature is much increased as the result of its high absorption of $CO_2$ laser radiation. The evidence for the presence of different products of $SF_6$ dissociation comes from the IR spectra – not shown – of the exhaust gases ($CF_4$: 1282 $cm^{-1}$ with a possible superposition of $N_2O$: 1265 $cm^{-1}$, $SiF_4$ with two maxima at 1028-1035 $cm^{-1}$, $CS_2$ ; 1530-1541 $cm^{-1}$,….) or from investigations with a TEM with an energy-dispersive X-ray spectrometer. Some quantitative chemical analysis of the soot revealed quite a large quantity of sulfur. The amounts of sulfur and fluorine in soot ( 28-50 % S and 3.5-7 %F) and also the black solid phase (residue) separated after the toluene extraction are higher for samples having lower C/F atomic ratio; this probably derives from the higher temperature and more decomposition of $SF_6$. That there was less sulfur in the residue (~ 6%) shows that most of it passes into solution during extraction with toluene. This presence in practically all steps of soot processing suggests diverse states of sulfur, from possibly free sulfur as $S_8$ up to, probably, new family of heteromolecular solids[7] with the general formula $C_{2n}(S_8)_m$, which combine $S_8$ zigzag rings with fullerene molecules in a solid with strong covalent intramolecular and weak, predominantly Van der Waals, intermolecular bonding. Investigations by transmission electron microscopy (TEM) show that curved structures are a general feature of the morphology of carbons; the soot is made of small particles, most of which coalesce each other forming chains. Particle shape seems to be rather spherical (Figure 1a), with a size distribution that covers a relatively narrow domain. The main dimension, depending on the gas mixture, is situated in the range of 50 and 10 nm. The larger diameter (~ 45 nm) is obtained in the case of ethylene pyrolysis and continuously decreases if the gas mixture is hydrocarbon/$C_2H_4$ (~30-35 nm, fig. 1c and d), hydrocarbon/$SF_6$ (~20-30 nm, fig. 1 e) or hydrocarbon/$SF_6$/$N_2O$ (< 20 nm, fig. 1f)[8]. Especially worth noting is the significant influence of the flame temperature, which must be correlated with the concentration of sensitizer and/or oxidizer as well as laser power. Higher temperature leads to higher amount of carbon atoms available for saturation of the free radicals and consequently to very small graphitic layers and basic structural units. It increases $SF_6$ dissociation and the presence of sulfur, fluorine or fluorinated radicals could limit the growth process by end-capping the intermediate radicals involved in soot formation or modify the particles' morphology. Investigations with a TEM coupled with an EDX spectrometer have shown higher sulfur concentration for belonging smaller carbon particles than for bigger ones. Oxidation reactions could be also responsible for the smaller particles dimension resulted in the case of an oxygen-containing gas mixture as well as for the soot morphology change from a turbostratic structure to a fullerene-like one. Although the appearance of the particles is disordered, an underlying graphitic structure may be put into evidence by presence of diffuse halo in the electron diffraction pattern (SAED) - not shown - or observed by X-ray diffraction investigations.

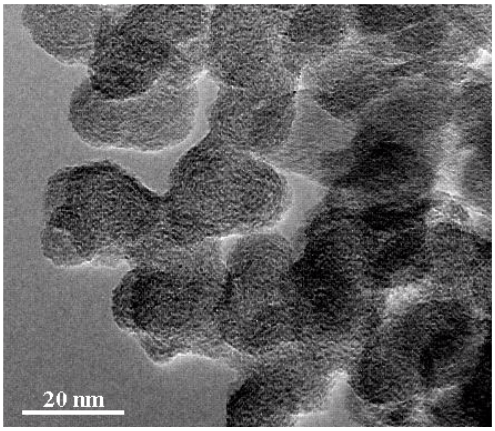


a.

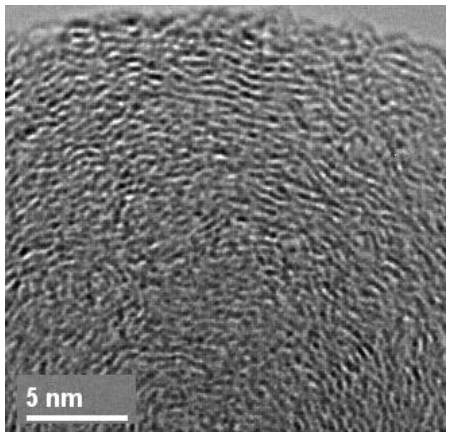


b.

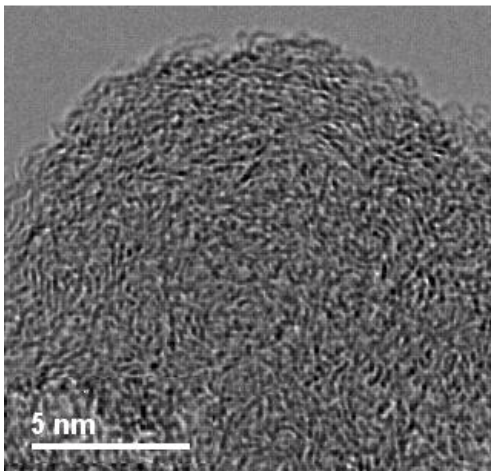


c.

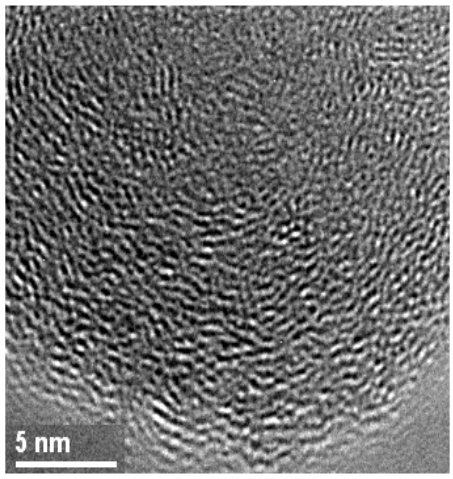


d

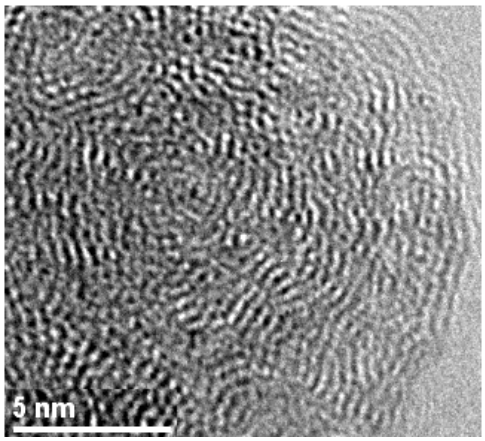


e.

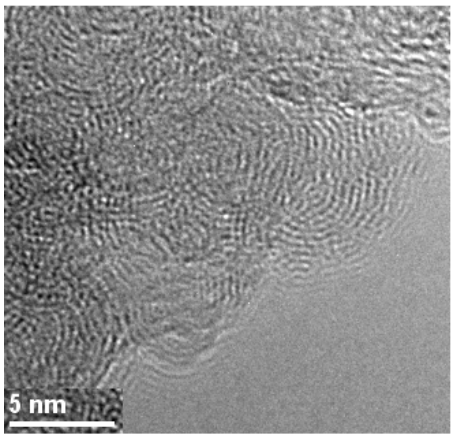


f.

Fig. 1. TEM images of carbon soot synthesized from: a. and b.: $C_2H_4$, c.: $C_2H_2$ with $C_2H_4$ as sensitizer, d.: $C_6H_6$ with $C_2H_4$ as sensitizer, e.: $C_6H_6$ with $SF_6$ as sensitizer, f.: $C_6H_6/N_2O$ with $SF_6$ as sensitizer.

Curvature of carbon layers seen in high resolution transmision electron microscopy (HRTEM) images (Fig. 1) was quantified by measuring the arc length L and arc diameter D of many layers and computing a curvature parameter defined by Goel at al.[9] as $C = L/\pi D$ which ranges from 0 for a

planar layer to 1 for a completely closed spherical layer. The results shown in Table 1 indicate that an increase of curvature parameter is achived by increasing of the arc length L or/and decreasing of diameter D. The values of curvature are banding between 0, which may corespond to a Highly Orientated Pyrolitic Graphite (HOPG) material and 1 which may corespond to fullerenes,onion like structures or nanoparticles covered by carbon shells.

Table 1. The computing curvature of carbon nanoparticles synthesized by laser pyrolysis of different reactive gas mixtures

| Gazeous mixture | Arc diameter D [nm] | Arc length L [nm] | Curvature C | La [Å] |
|---|---|---|---|---|
| $C_2H_4$ | 6.1 | 3.7 | 0.20 | 18-19 |
| $C_2H_2/C_2H_4$ | 6.1 | 2.1 | 0.10 | 19-20 |
| $C_6H_6/C_2H_4$ | 9.5 | 5.3 | 0.18 | - |
| $C_6H_6/SF_6$ | 5.1 | 6.0 | 0.37 | 16-17 |
| $C_6H_6/SF_6/N_2O$ | 2.1 | 1.7 | 0.26 | 17-18 |

As it could be seen from the Table 1, when $C_2H_4$ or $C_2H_2/C_2H_4$ is used as precursor, the carbon layers lay on an almost constant arc diameter (~6 nm). This mean value increases to aproximately 9.5 nm in the case of $C_6H_6/C_2H_4$ gas mixture. Noting the larger arc diameter in this last case, the use of $SF_6$ in a $C_6H_6/SF_6$ mixture diminishes the arc diameter with about 40 % (5.1 nm) and, by increasing the arc length to higher values (6 nm), stresses the curvature, C. The same behavior could be observed in the case of $C_6H_6/SF_6/N_2O$ mixture. These observations suggest the bending role of graphene layers by $SF_6$ and $N_2O$ and, at least in this last case, the tendency to form carbon structures characterized by a high degree of curvature. On the other hand, the arc length, L, is clearly larger in the case of benzene-based mixtures: ethylene addition leads to an increase of arc length, L, while that of $SF_6$ seems to leave this parameter unchanged. The use of $N_2O$ leads to an accentuated decrease of both arc diameter and length. This observations show an important influence of $SF_6$ and $N_2O$ on the morphology of carbon soot synthesized by the laser pyrolysis process based on a high temperature C/H/O system. Noting the crucial role of oxygen in the mechanism of fullerene formation[10], we suppose that the fluorine diffusion between graphene layers accentuates their curvature, and implicitly the curvature increasing with the quantity of intercalated fluorine. The XRD patterns of the greatest part of the samples reveal the two broad diffraction peaks located at $2\theta \sim 25^o$ and $\sim 43^o$, indexed respectively as (002) and (10) in accordance with the turbostratic structure[11]. The maximum corresponding to (002) planes shows that graphene sheets are already formed and organized as parallel layers spaced at a relatively well-defined interplanar distance $d_{002}$. The XRD and Raman spectrometry investigations allow to deduce important structure parameters: $d_{(002)}$ – the average distance between the graphite layers, $L_c$ - the average stacking height in the direction perpendicular to the graphene layers, and $L_a$ – crystalline size in the plane of graphene layers. Some salient experimental conditions and results, for the runs using different gas mixtures, are presented in Table 2. It is worth noting that the analysis of XRD spectra of the samples obtained from different precursors and in different experimental conditions shows different low angle shifts for the maximum assigned to graphitic planes (002).

Table 2. Experimental data and results obtained in runs with different gas mixtures.

| Run | Gas composition and volume ratio | $P_L$ [W] | P [mbar] | (C/F) at. ratio | (C/O) at. ratio | $d_{002}$ [Å] | $L_a$ [Å] | 2θ [degree] |
|---|---|---|---|---|---|---|---|---|
| AS69 | $C_2H_2/SF_6$ , 1.5 / 1 | 700 | 750 | 0.5 | - | 3.89 | 18.9 | 23.1 |
| AS70 | $C_2H_2/SF_6$ , 2.4 / 1 | | | 0.8 | - | 4.45 | 18.1 | 20.0 |
| AS71 | $C_2H_2/SF_6$ , 4.4 / 1 | | | 1.5 | - | 3.77 | 18.4 | 24.0 |
| AS72 | $C_2H_2/SF_6$ , 9 / 1 | | | 3 | - | 3.58 | 20.5 | 24.9 |
| AS99 | $C_2H_2/SF_6$ | 800 | 750 | 0.8 | - | - | 18.9 | - |
| AS100 | $C_2H_2/SF_6$ | | | 0.5 | - | - | 20.9 | - |
| AS101 | $C_2H_2/SF_6$ | | | 1.5 | - | - | 19.1 | - |
| AS102 | $C_2H_2/SF_6$ | | | 3 | - | - | 21.6 | - |
| BS73 | $C_6H_6/SF_6$ , 1 / 2 | 800 | 750 | 0.5 | - | 3.67 | | 24.3 |
| BS74 | $C_6H_6/SF_6$ , 1 / 2.6 | | | 0.4 | - | 3.67 | 20.0 | 24.3 |
| BS83 | $C_6H_6/SF_6$ , 1 / 0.84 | | | 0.8 | - | 3.71 | | 23.7 |
| BSO81 | $C_6H_6/SF_6/N_2O$,1/2 / 6 | 800 | 750 | 0.5 | 1 | 3.58 | 12 | much S |
| BSO82 | $C_6H_6/SF_6/N_2O$, 1/1.24/6 | | | 0.81 | 1.2 | 3.74 | | 23.8 |
| BSO92 | $C_6H_6/SF_6/N_2O$, 1/1.24/6 | | | 0.8 | 1.2 | 3.62 | | 24.6 |
| BE85 | $C_6H_6/C_2H_4$ , 1 / 0.6 | 800 | 750 | - | - | 3.64 | - | 24.6 |
| BE87 | $C_6H_6/C_2H_4$ , 1 / 2.77 | | | - | - | 3.65 | - | 24.3 |
| BE88 | $C_6H_6/C_2H_4$ , 1 / 1.85 | | | - | - | 3.63 | - | 24.6 |

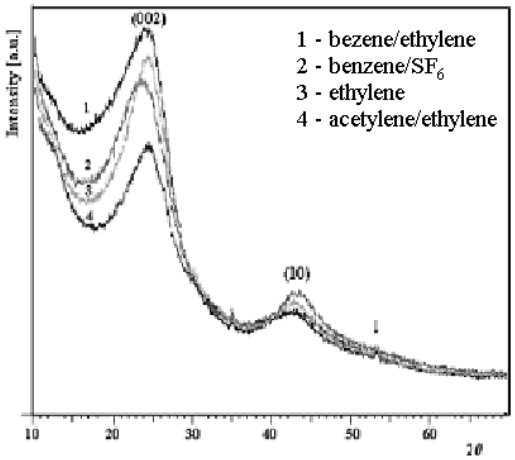


Figure 2. XRD spectra of samples obtained from benzene/ethylene (curve 1), benzene/sulfur hexafluoride (curve 2), ethylene (curve 3), and acetylene/ethylene (curve 4).

These shifts suggest the increase of the mean distance between respective planes. Figure 2 presents the XRD spectra of four samples obtained by laser pyrolysis of benzene/ethylene (curve 1), benzene/sulfur hexafluoride (curve 2), ethylene (curve 3) and acetylene/ethylene (curve 4). Larger low angle shift corresponding to the maximum assigned to (002) planes for the sample obtained from a $C_6H_6/SF_6$ mixture, compared to almost the same position of the (002) band from spectra 1, 3, and 4, suggests that the interplanar distance $d_{002}$ increases significantly when sulfur hexafluoride is introduced into the gas mixture. The ratio hydrocarbon/sulfur hexafluoride flow rates is expected to be directly responsible for the temperature of the reaction flame and fluorine and sulfur concentration and therefore it influences the structural, chemical or morphological properties of the synthesized soot. For the runs using $C_2H_2/SF_6$ mixtures with different C/F atomic ratio (experiments AS69 – AS72) the

maximum assigned to (002) planes is situated at $2\theta \sim 23.1^{o}$, $20.0^{o}$, $24.0^{o}$ and $24.9^{o}$, respectively (Figure 3a). The size of these shifts seems to be influenced by $SF_6$ concentration, suggesting the increase of the mean distance between (002) planes (Figure 3b).

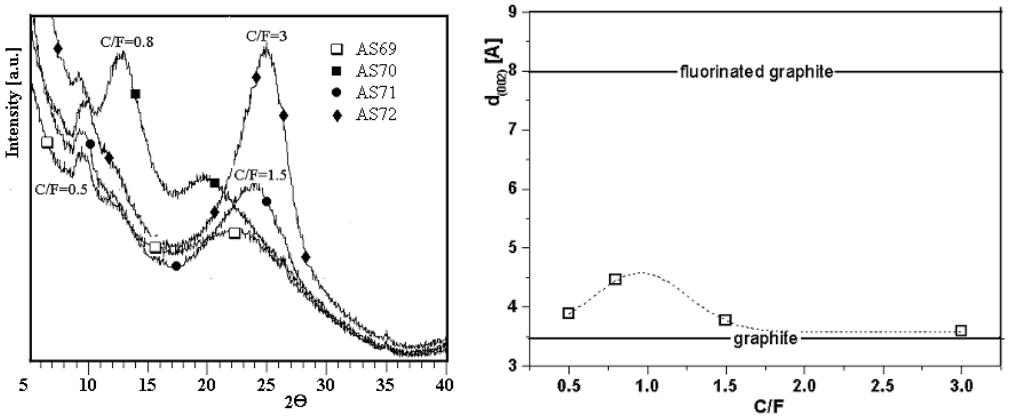


a) b)

Figure 3 a) XRD spectra of samples obtained from $C_2H_2/SF_6$ mixtures with different (C/F) at ratios, b) the mean distance between (002) planes of the carbon nanopowder synthesized in these experiments

This change could be provoked by the presence of sulfur and fluorine released by $SF_6$ decomposition (e.g. 28% S and 7% F were quantified in sample BS74). The affirmation seems to be in good agreement with previous studies[12 – 16], showing that fluorine has a dual ionic and covalent behavior in graphite and the chemical composition of fluorinated carbons depends on both the structure of the starting material and the fluorination conditions. It is supposed that the structure of the fluorinated graphite is layered and is derived from graphite by insertion of covalently bonded fluorine atoms above and below every hexagon in each layer. Concurrently, by heating the graphite fluoride in the presence of sulfur, the majority of the fluorine atoms appeared to leave the structure without reacting with carbon atoms; some sulfur appeared to replace fluorine and be attaching to the carbon structure. This could explain the anomalous behavior of the sample AS 69 , with a C/F ratio ~0.5 (Fig. 3b), with an unexpected smaller $d_{002}$ value, when , in spite of a higher concentration of fluorine, the abundant presence of sulfur decreases the number of C-F bonds; the interplanar distance increases when $SF_6$ is introduced in the gas mixture, reaches a maximum and then slowly decreases with the increase of $SF_6$ concentration.

The two Raman features (G band of crystalline graphite and D band) could be a measure of the degree of order in an amorphous carbon sample. The $I_D/I_G$ ratio was found to correlate with the graphitic order, well described by the crystalline size, $L_a$, in the plane of the graphene layers[17]. These $L_a$ values are situated generally in the range of 15-25 Å and present a slight increase trend both with laser power and working pressure. Raman measurements performed on soots synthesized by using $C_2H_2/SF_6$ mixtures with different C/F atomic ratio (runs AS69 – AS72) present a good correlation between $L_a$ values

and the shifts of (002) peak (Fig. 4 a), and indirect, between $L_a$ and the distance, $d_{(002)}$.

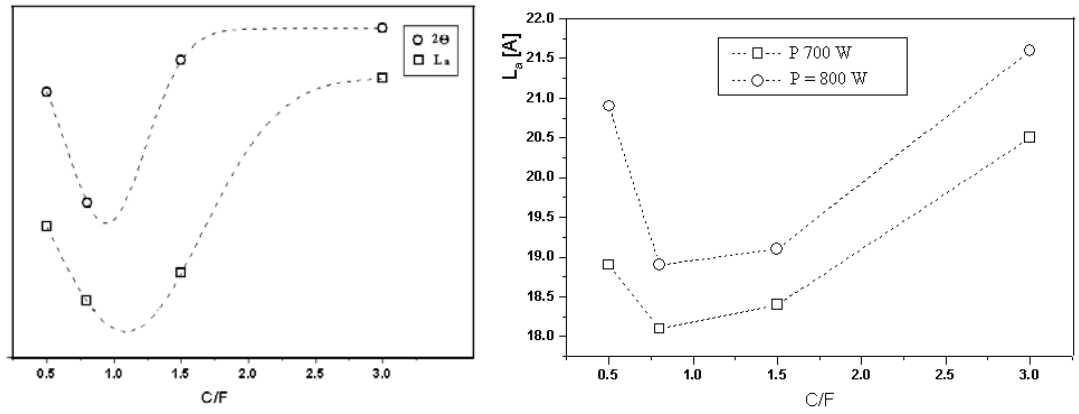


a. b.

Figure 4 a. The variations of $L_a$ and low angle shifts (2θ) for runs with different C/F ratios; b. The dependence $L_a$ vs. (C/F) at. ratio for two series of identical experiments performed at different laser power.

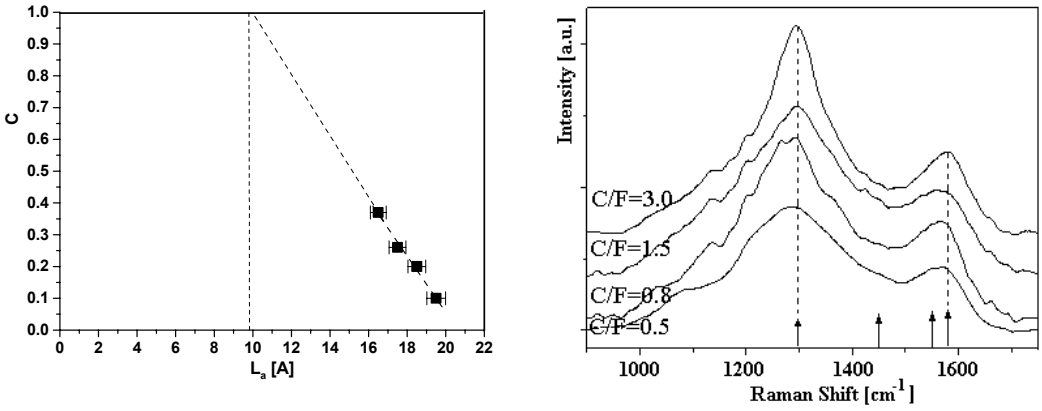


a. b.

Figure 5. A. The dependence between crystalline size $L_a$ and curvature C; b. Raman spectra of samples obtained from a $C_2H_2/SF_6$ gas mixture of different C/F atomic ratio

Also, $L_a$ values seem to increase at the higher laser power as it could be observed in Figure 4 b, where the dependence $L_a$ vs. (C/F)at. ratio for two series of identical experiments (AS69-AS72 and AS99-AS102) performed at different laser power (700 and 800W, respectively), was represented. From the data resulted in the frame of the exploratory experiments, it results that a good correlation may be established between $L_a$ and C values obtained for some samples synthesized from different gas mixtures and having different structures. The variation of $L_a$ parameter is given mainly by pressure and laser power variation and shows to be linear dependent of curvature C, which riches the maximum value of 1 at $L_a$ ~ 10 nm (Figure 5a). In agreement with the previous published data[18], Raman spectra of the experiments with different C/F atomic ratio (the same $C_2H_2/SF_6$ mixture) are shown in Figure 5b. The data show the presence of two lines inside the G band centered at ~ 1580 $cm^{-1}$, the D band at ~ 1300 $cm^{-1}$ and a large band at about 1450 $cm^{-1}$. With

increasing values of fluorine concentration, the frequency of the line centered on the D band does not change much, while the doublet inside the G band shows the slight downshift in frequency. In accordance with the findings of the other authors[19], the Raman spectrum of Highly Oriented Pyrolytic Graphite upon intercalation with acceptors shows one or two lines function of the fluorination degree; previous TEM studies[20] on dilute fluorine-intercalated graphite showed the presence of high fluorination compounds and unintercalated graphitic regions. Sample inhomogeneities could in part be responsible for the broad peak[21] from ~1450 $cm^{-1}$. The observed modifications of the D band indicate clustering of the $sp^3C$ aromatic rings with increasing concentration of sulfur[16].

## 4. Conclusions

In the no resonant processes of gas phase laser pyrolysis, the sensitizer ($SF_6$) undergoes different degrees of dissociation and can either react or interfere through its decomposition products. Soot's investigations showed that the curved structures are the general features of the morphology of carbons. This morphology could be altered by the heterogeneous atoms like oxygen or fluorine and sulfur. Partial fluoridation of the carbon nanopowders is produced during the synthesis process. This fluoridation could be diminished by the concurrently presence of sulfur. There is a closed correlation between the main important experimental parameters (precursor's nature, temperature, and pressure), oxygen, fluorine, and sulfur concentration and the morphology of the synthesized carbon nanopowder.

## Acknowledgements

The authors gratefully acknowledge financial support from NATO under project NATO SfP-974214 and from the Romanian Ministry of Education and Research under contract RO 99 404

## References

1. J.B. Howard, J.T. McKinnon, Y. Makarovsky, A.L. Lafleur and M. E. Johnson, "Fullerenes $C_{60}$ and $C_{70}$ in Flames", Nature 352, pp. 139 -141, 1991
2. M. Ebrecht, M. Faerber, F. Rohmund, V.V. Smirnov, O. Stelmach and F. Huisken, "CO2-Laser-Driven Production of Carbon Clusters And Fullerenes From The Gas Phase", Chem. Phys. Lett. 214, 1, pp. 34-38, 1993
3. I. Voicu, X. Armand, M. Cauchetier, N. Herlin and S. Bourcier, "Laser synthesis of fullerenes from benzene-oxygen mixtures", Chem. Phys. Lett. 256, pp. 261-268, 1996
4. C. Vahlas, A. Kacheva, M.L. Hitchman and Ph. Rocabois, "Thermodynamic Study of Formation of $C_{60}$ and $C_{70}$ by Combustion or Pyrolysis", Journal of the Electrochemical Society 146, 7, pp. 2752-2761, 1999
5. R. Alexandrescu, X. Armand, M. Cauchetier, N. Herlin, S. Petcu and I. Voicu, "Effect of $SF_6$ addition in the laser synthesis of fullerene and soot from $C_6H_6/O_2$ or $C_6H_6/N_2O$ sensitized mixtures", Carbon 36, 9, pp. 1285-1290, 1998

6. Bauer RA, Smulders S, Becht JGM, Van der Put PJ and Schoonman J, J. Am. Ceram. Soc. 1989;72: 1301
7. Roth G, Adelmann P, The crystal structure of C70S48 – The 1st A-Priori Structure Determination of a C70-Containing Compound, Journal de Physique I 1992;2 (8):1541-1548
8. Morjan I, Voicu I, Alexandrescu R, Pasuk I, Sandu I, Dumitrache F, Soare I, Fleaca TC, Ploscaru M, Ciupina V, Daniels H, Westwood A and Rand B, Gas composition in laser pyrolysis of hydrocarbon-based mixtures; influence on soot morphology, Carbon 2004, in press
9. Goel A, Hebgen P, Vander Sande J B, Howard JB, Combustion synthesis of fullerenes and fullerenic nanostructures, Carbon 2002; 40: 177-182.
10. R.A. Shandross, J.P. Longwell, J.B. Howard, "Destruction of benzene in high-temperature flames: chemistry of benzene and phenol", Twenty Sixth Symposium (International) on Combustion, The Combustion Institute, Pittsburg 1996, pp. 711-719
11. Shen Zhu, Ching-Hua Su, Cochrane J.C., Lehoczky S., Muntele I., Ila D., Growth of Carbon Nanostructure Materials Using Laser Vaporization, Diamond and Related Materials 2001; 10: 1190-1194
12. di Vittorio SL, Dresselhaus MS, Dresselhaus G, A model for disorder in fluorine-intercalated graphite, J. Mater. Res., 1996; 8 (7):1578
13. Kurmaev EZ, Moewes A, Ederer DL, Ishii H, Seki K, Yanagihara M, Okino F and Touhara H., Electronic structure of graphite fluorides, Physics Letters A 2001;288: 340-344
14. Tressaud A, Shirasaki T, Nansé G, and Papirer E, Fluorinated carbon blacks: influence of the morphology of the starting material on the fluorination mechanism, Carbon 2002; 40: 217-220
15. Kelly KF, Mickelson ET, Hauge RH, Margrave JL, and Halas NJ, Nanoscale imaging of chemical interactions: Fluorine on graphite, PNAS 2000; 97 (19): 10318-10321
16. Filik J, Lane IM, May PW, Pearce SRJ, and Hallam KR, Incorporation of sulfur into hydrogenated amorphous carbon films, Diamond and Related Materials, 2003, in press
17. Ferrari A.C. and Robertson D., Multi-wavelength Raman Spectroscopy of Carbon, Phys. Rev. B 2000; 61: 14095
18. Rao AM, Fung AWP, di Vittorio SL, Dresselhaus MS, Dresselhaus G, Endo M, Oshida K, and Nakajima T, Raman-scattering and transmission-electron-microscopy studies of fluorine-intercalated graphite fibers CxF, Physical Review B, 1992;45 (12); 6883-6892
19. Dresselhaus MS and Dresselhaus G, in Light Scattering in Solids III, edited by M. Cardona and G. Güntherodt, Topics in Applied Physics Vol. 51 (Springer Verlag, Berlin, 1982), p.3
20. Nakajima T, Watanabe N, Kameda I, Endo M, Carbon 1986;24; 343
21. Ohana I, Palchan I, Yacoby Y, Davidov D, Solid State Commun. 1985;56: 505